

POINT DEFECTS IN B2 INTERMETALLIC COMPOUNDS

Gary S. Collins, Praveen Sinha and Mingzhong Wei *

Department of Physics, Washington State University, Pullman, WA 99164, USA

We are applying perturbed angular correlations (PAC) to study point defects near ^{111}In probes in ordered B2 alloys. Systems studied include NiAl, CoAl, FeAl, CoGa and PdIn. Ten different point defect configurations have been observed in annealed, quenched or mechanically-milled samples. The present status of this work is summarized. Systematics of hyperfine interactions of vacancy defects are then examined. It is found that quadrupole interactions due to first-shell transition-metal vacancies vary in good approximation as the reciprocal cube of the lattice-parameter. Quadrupole interactions due to configurations of two first-shell vacancies exhibit deviations from predictions of a simple point-charge model, which can be explained by small amounts of local lattice relaxation of the probe atom toward the vacancies, of order 0.02 nm.

The intermetallic compounds NiAl, CoAl and FeAl are under active investigation as structural materials for high-temperature applications. These are all highly-ordered compounds with the B2 (CsCl) phase extending over broad compositional ranges. All of them, as well as other B2 systems formed by combining a transition metal (T) with a trivalent element (B), such as CoGa and PdIn, are known to accommodate deviations from stoichiometry, in annealed samples, with transition-metal vacancies (V_T) for T-deficient alloys and transition-metal antisite atoms (T_B) for T-rich alloys. In this laboratory, we have been applying the method of perturbed angular correlations of gamma rays (PAC) to investigate defect properties in such compounds. The point defects are detected when they localize within a few atomic shells near ^{111}In probe atoms through nuclear quadrupole interactions induced at (daughter) ^{111}Cd probe nuclei. We have studied *annealed* (A) samples, to observe structural defects that accommodate deviations from stoichiometry, *quenched* (Q) samples, to observe high-temperature equilibrium defects, and *mechanically-milled* (M) samples, to observe other, higher-energy, point defects. Here, the present status of these studies is first summarized. Then, hyperfine interactions of equivalent defects in the different compounds are compared.

Experimental methods.

Samples within a few percent of stoichiometry, on either side, were prepared by arc-melting high purity metals and ^{111}In probe activity together (the mole fraction of ^{111}In was always of order 10^{-8}). Annealing was carried out at the lesser of 1200 C or 100 C below the melting temperature, followed by slow cooling to room temperature. Quenched samples were equilibrated for one hour in a vertical tube furnace and then dropped into a cooling bath at room temperature. Milled samples were attrited in a Spex 8000 mill using steel or WC vials. PAC spectra were measured using a standard four-counter spectrometer with BaF_2 scintillators, and spectra were fitted with a superposition of perturbation functions due to static quadrupole interaction. For each function, the fundamental measured perturbation frequency, ω_1 , asymmetry parameter of the electric-field gradient tensor, η , and site fraction f were obtained. Further details on methods used are in ref. [1].

Defect identification

Signals detected in the five alloys have been identified with about ten different, discrete, local defect environments. One can be quite certain that the In probe will localize on the B-sublattice in these systems since it is isovalent with B and since the structural defect in T-deficient alloys is V_T and not B_T , indicating that B_T is a high-energy defect. *A fortiori*, the large In atom radius should make In_T an even higher-energy defect. Quadrupole interaction strengths induced by defect charges fall off as $1/r^3$

with distance, if one neglects screening of the conduction electrons, so that defects in the first few shells around the In_B probe should have the largest interactions; the first four shells belong to the T,B,B, and T sublattices of the B2 structure. Common defect configurations to which signals have been attributed are shown in Fig. 1.

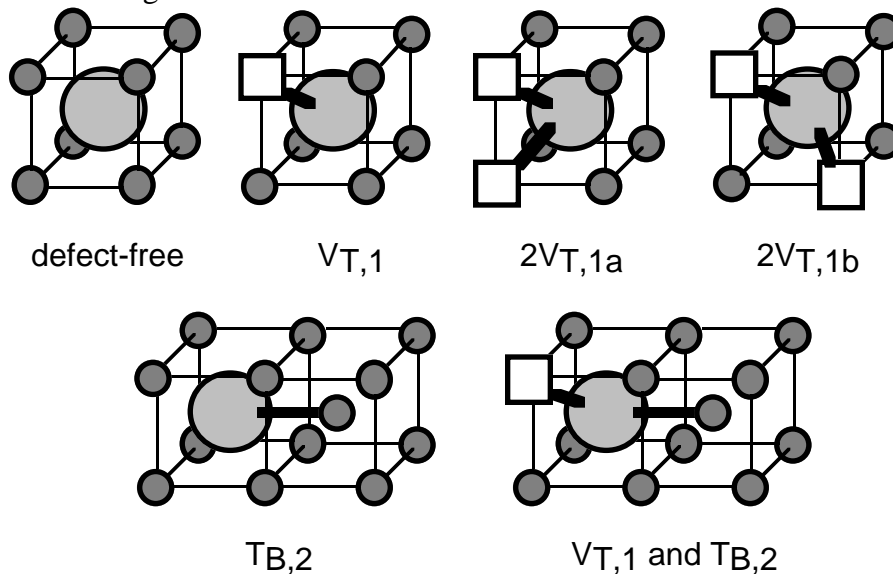


Fig. 1. Local defect configurations near In-probe atoms (large circles). Small circles and squares represent transition-metal atoms and transition-metal vacancies.

First-neighbor T-metal vacancies. For NiAl,[2,3] CoAl [3] and PdIn,[4,5] V_T signals were identified from measurements on annealed, T-deficient samples, for which V_T defects are expected, and/or on quenched, T-rich samples, for which V_T was an expected constituent of the high-temperature equilibrium defect. From changes in site fractions of V_T with composition (T-deficient alloys) or quenching temperature (T-rich alloys), signals were identified with one V_T defect in the first-neighbor shell ($V_{T,1}$) and two V_T defects in the first shell in two distinct configurations ($2V_{T,1a}$, $2V_{T,1b}$). (See Fig. 1; numerical subscripts identify the shell numbers). It was not possible to identify vacancy signals in FeAl [3] and CoGa [6] in the same way because local vacancy concentrations next to In probes are so large that systematic trends are obscured. However, both alloys exhibit prominent signals whose hyperfine parameters are quite similar to those of $V_{T,1}$ and $2V_{T,1}$ for the first three alloys, and so have been similarly identified.

Other defect configurations. The hyperfine interactions for all defect-configurations identified to date are listed in Table 1. Seven defect configurations not described above are listed, including: the structural antisite defect, $T_{B,2}$ in T-rich alloys; a low-frequency signal in annealed, Pd-deficient, PdIn identified with the fourth-shell vacancy $V_{T,4}$; a signal in Pd-rich, quenched PdIn attributed to a second or third shell In-vacancy; a high-energy antisite configuration $\text{In}_{Pd,1}$ in milled PdIn; and two configurations involving the combination of a first-shell vacancy with another defect. Further details about identification will be found elsewhere.

Defect properties.

Properties of equilibrium high-temperature defects in NiAl, CoAl and PdIn have been obtained from studies of quenched samples. For these alloys, the site fraction f_I of $V_{T,1}$ increases with quenching temperature due to an increasing thermal-defect concentration. The thermal defect was identified as the Schottky vacancy-pair in NiAl (and not the so-called triple defect) from the observation that the quenched-in vacancy site fraction is independent of alloy composition.[3,7] For NiAl (and CoAl,

whose defect behavior is similar) the formation enthalpy E_F and entropy of the Schottky defect were determined from an Arrhenius plot of the “renormalized” monovacancy site fraction, $f_1/(1-f_1-f_2)$. Using a methodology we developed that applies the law of mass action, accounts for the binding enthalpy of V_T to the impurity In probe, and allows for local motion of defects during the quench, it can be shown that the activation enthalpy $Q = E_F/2$. [7,8] Results obtained for NiAl and CoAl were, respectively, $E_F = 2.22(8)$ eV and $3.10(12)$ eV. The Schottky defect was determined to be the thermal defect in PdIn through observations of parallel increases in site fractions of V_{Pd} and V_{In} defects with increasing quenching temperature; the Schottky-defect formation enthalpy was determined to be $E_F = 2Q = 1.3(2)$ eV from an Arrhenius plot of the concentration of V_{Pd} . [4]

Table 1. Defect configurations near In probes in five B2 alloys. Column 2 indicates if the configuration has been observed in annealed, quenched or milled samples. Column 3 lists theoretical values for the interaction frequency ω_1 (arbitrary scale) and η estimated using a simple point-charge approximation. Columns 4-8 list measured values of the frequency ω_1 , in Mrad/s, and η for each configuration.

Defect Config.	Observed	Theory	NiAl	CoAl	FeAl	CoGa	PdIn
$V_{T,1}$	A Q M	1, 0	128, 0	144, 0	141, 0	137, 0	103, 0
$BT_{,1}$	- - M		-	-	-	-	69, ~0.6
$TB_{,2}$	A Q -		19, ~0	21, ~0	-	-	34, 0
$VB_{,2}$ or $VB_{,3}$	- Q -		-	-	-	-	~17, ~0
$VT_{,4}$	A Q -	0.14, 0	-	-	-	-	~6, ~0
$2V_{T,1}$ (a,b)	A Q M	1.76, 1 1.76, 1	187, 0.64 222, 0.89	223, 0.51 280, 0.78	-	193, 0.69 293, 0.95	163, 0.68 194, 0.80
$2V_{T,1}$ (c)	A - -	2, 0	-	-	-	218, 0	-
$V_{T,1}$ and $TB_{,2}$	- Q -		141, ~0.2	153, ~0.2	-	-	-
$V_{T,1}$ and $V_{T,4}$	A - -		-	-	-	-	112, ~0.2

Migration enthalpies E_M of T-metal vacancies in NiAl, CoAl and PdIn have been determined to be 1.7(2) eV, 2.1(2) eV and 1.7(2) eV, respectively, from measurements of the temperatures at which quenched-in vacancies are observed to anneal out, assuming random diffusion of the vacancies and using estimates of quenched-in defect concentrations. Finally, binding enthalpies E_B to In probes of V_T defects in NiAl and CoAl were determined to be 0.22(1) eV and 0.19(1) eV, respectively, from measurements in a low temperature regime in which the vacancies could move but not anneal out. [3] (E_B for PdIn is, of course, zero because the In probe is not an impurity in that system).

Hyperfine interactions of vacancy defect configurations.

We examine measured hyperfine interaction parameters ω_1 and η to determine what information they provide about the defect configurations. In general, interaction parameters may be expected to depend on the effective charges of the elementary defects, their distances from the probe atom, and changes in distances and angles due to local lattice relaxations. Measured interaction frequencies for configurations $V_{T,1}$ in the five alloys are plotted versus the lattice parameters in Fig. 2, with the drawn curve showing a $1/r^3$ dependence. Good agreement between the data points and curve supports a $1/r^3$ dependence and suggests that effective charges of T-metal vacancies in the five alloys are equal within about 10%.

Lattice relaxation should be more important in multivacancy configuration such as $2V_{T,1(a,b)}$. To provide a benchmark for comparison with the measurements, interaction frequencies ω_1 and η were calculated for the vacancy configurations in Table 1 using a point-charge defect approximation, with results shown in column 3 of Table 1. As can be seen, both $2V_{T,1}$ configurations are expected to have the same hyperfine interactions, with the normalized frequencies $\omega_1(2V)/\omega_1(1V) = 1.76$ and $\eta = 1$. Experimental values of $\omega_1(2V)/\omega_1(1V)$, normalized in the same way to eliminate variations due to differences in lattice parameter or effective vacancy charge, are plotted in Fig. 3. The mean value of $\omega_1(2V)/\omega_1(1V)$ is observed to be in excellent agreement with the theoretical value 1.76. The differences are attributed to lattice relaxation, which is expected to be greater for configuration $2V_{T,1a}$ than for $2V_{T,1b}$ because in the latter case, as can be seen from Fig 1, the two T-metal atoms on opposite

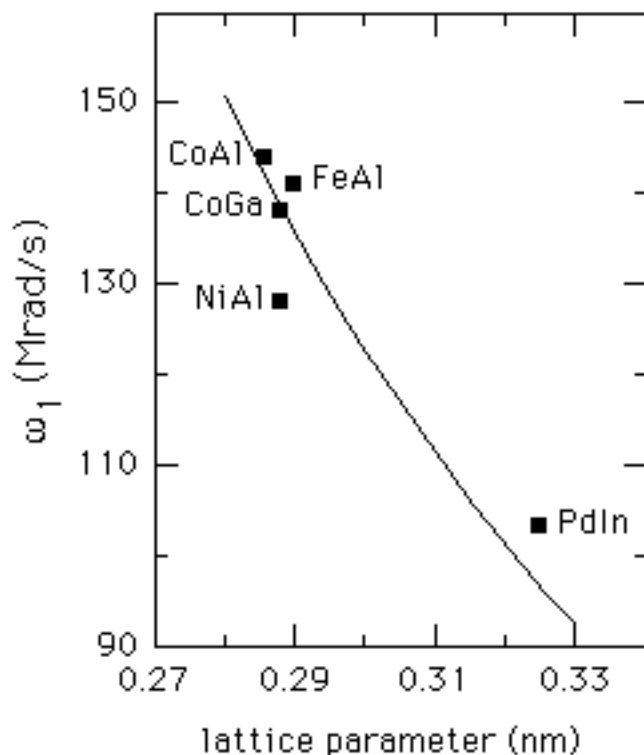


Fig. 2. Interaction frequencies of first-shell vacancies in five B2 alloys plotted versus the lattice parameter. The drawn curve shows a reciprocal-cube dependence.

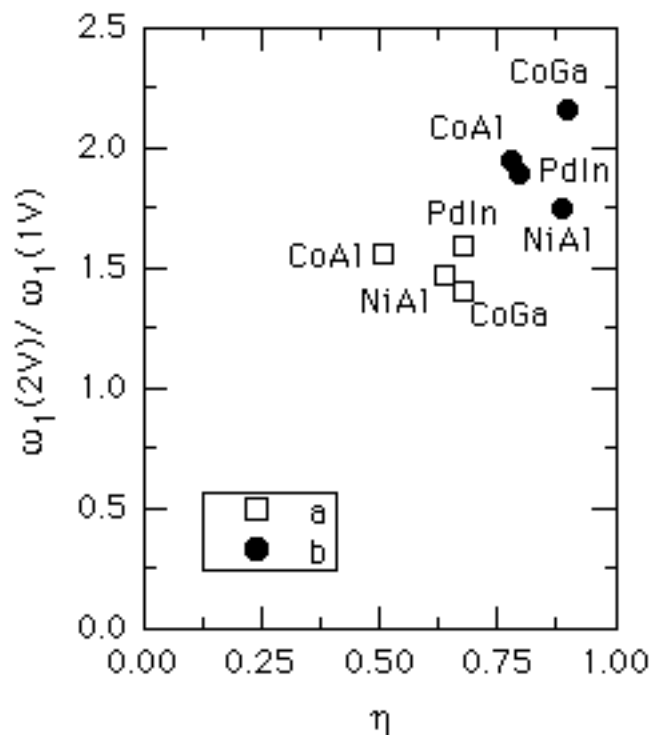


Fig. 3. Hyperfine interactions of first-shell divacancy configurations (a) and (b).

corners of the cube face provide more steric constraint against displacement of the In probe. (Indeed, sites a and b were originally labeled for each alloy so that site a exhibited the greater deviation from $\eta = 1$.) The probe atom is expected to relax toward the two vacancies in both cases. In order to estimate the magnitude of relaxations necessary to explain the data, we carried out simple point-charge calculations of the electric-field gradient induced by two identical defect charges at equal distances from a probe atom and spanning a variable angle θ . It was found that the mean $\eta \approx 0.63$ of values for configuration a can be obtained by increasing θ from the ideal (unrelaxed) value of 70.5° by only 7° . For configuration b, the mean $\eta \approx 0.83$ can be obtained by increasing θ by only 4° from the ideal value of 109.5° . Within the framework of this simple model, it can be shown that such angular changes may be produced by displacements of the probe atom toward the center of gravity of the two vacancies by distances of about 0.04 nm and 0.015 nm for configurations a and b, respectively. The model therefore

suggests that modest lattice relaxations are able to account for deviations of the asymmetry parameters of the 2V configurations from unity.

References

* Supported in part by the National Science Foundation under grants DMR 90-14163 and 93-13702 (Metals Program).

1. G. S. Collins, S. L. Shropshire and J. Fan, *Hyperfine Interactions* 62 (1990) 1.
2. Jiawen Fan and Gary S. Collins, *Hyperfine Interactions* 60 (1990) 655.
3. Jiawen Fan, PhD dissertation, Washington State University, 1992 (unpublished).
4. Praveen Sinha and Gary S. Collins, *Mat. Res. Soc. Symp. Proc.* 364 (1995) 59.
5. Praveen Sinha, PhD dissertation, Washington State University, 1995 (unpublished).
6. Ming-Zhong Wei, Bin Bai and Gary S. Collins, 1995 (unpublished).
7. Gary S. Collins and Jiawen Fan, 1993 (unpublished).
8. The methodology in ref. 7 treats local motion of defects during the quench, which was not considered in ref. 3 or in G. S. Collins and Jiawen Fan, *Hyperfine Interaction* 80 (1993) 1257. Present values for activation enthalpies supercede values reported previously in those references.